

Group A Rotavirus Associated with Encephalitis in Red Fox

Chiara Busi, Vito Martella, Alice Papetti, Cristiano Sabelli, Davide Lelli, G. Loris Alborali, Lucia Gibelli, Daniela Gelmetti, Antonio Lavazza, Paolo Cordioli,¹ M. Beatrice Boniotti

In 2011, a group A rotavirus was isolated from the brain of a fox with encephalitis and neurologic signs, detected by rabies surveillance in Italy. Intracerebral inoculation of fox brain homogenates into mice was fatal. Genome sequencing revealed a heterologous rotavirus of avian origin, which could provide a model for investigating rotavirus neurovirulence.

Group A rotaviruses are a major cause of diarrhea in humans and animals. Although group A rotaviruses infect particular species preferentially (homologous infection), they less frequently affect other species of mammals (heterologous infection), naturally and experimentally (1). In addition, there is evidence, albeit rare, that transmission of group A rotaviruses may occur between species of mammals and birds under natural and experimental conditions (2–4).

Group A rotaviruses have limited tissue tropism; infection is primarily restricted to cells of the small intestine. However, heterologous infection of mice with the rhesus group A rotavirus strain MMU 18006 was associated with extramucosal spread and hepatitis, but infections with bovine group A rotavirus WC3 and the homologous murine group A rotavirus EDIM were not (5), suggesting that some group A rotavirus strains may have unique or unexpected biological properties. In humans, group A rotavirus infection has been associated with acute encephalitis, although this association is based only on observational findings (6–9).

We detected a group A rotavirus strain in the brain of a fox with neurologic disorders. To determine the derivation of the virus, we further examined its genomic and biological features.

The Study

In 2011, as part of Italy's national surveillance program for rabies in wildlife, an adult red fox (*Vulpes vulpes*) with

neurologic signs was captured. Because its general condition worsened, the animal was euthanized and screened for a panel of neuropathogens (online Technical Appendix, <https://wwwnc.cdc.gov/EID/article/23/9/17-0158-Techapp1.pdf>). Test results indicated that the animal was negative for rabies, canine distemper, Aujeszky's disease, leishmaniasis, and flavivirus infection (online Technical Appendix). Following the standard diagnostic procedures for rabies, we inoculated brain homogenate from the fox intracerebrally into suckling and weanling mice. The suckling mice died after 3–4 days and the weanling mice after 5 days. However, immunofluorescence testing of the brains of all mice, using rabies-specific hyperimmune serum, produced negative results (data not shown).

Use of negative-staining electron microscopy revealed rotavirus-like virions in the fox and mouse brains (Figure 1, panels A, B). Histologically, several alterations/lesions, suggestive of acute inflammation, were observed in the cerebral cortex of the fox. Histologic analysis of gray matter revealed nonsuppurative encephalitis characterized by multifocal perivascular cuffing of lymphocytes, macrophages, and a few plasma cells as well as presence of multifocal small glial nodules. Perivascular accumulations varied from 1-cell thickness to thin cell accumulations (Figure 1, panel C). Neutrophils were observed within the lumen of some blood vessels and scattered in the gray matter. Neuronal necrosis and satellitosis were also present. By immunohistochemistry performed with a polyclonal serum raised against group A rotavirus, rotavirus antigen was detected in the cytoplasm of neurons, in dendrites, and in glial cells within inflamed areas of the brain (Figure 1, panel D).

An isolate, hereafter called fox-288356, was made from homogenates of the fox brain and from the brains of inoculated suckling and weanling mice, by using confluent monolayers of Marc-145 cells with and without trypsin. Cytopathic effect was characterized by foci of rounded cells, which tended to aggregate linearly on the surface of the monolayer and were clearly visible after 2 days (Figure 1, panel E). Electron microscopic observation identified rotavirus-like particles in the cell cryolysates (data not shown). The electropherotype of the cultured virus revealed a segmented genome characterized by a 5-1-3-2 profile with co-migration of segments 10 and 11 (online Technical Appendix Figure 1).

¹Deceased.

Author affiliations: Istituto Zooprofilattico Sperimentale della Lombardia e dell'Emilia Romagna "Bruno Ubertini," Brescia, Italy (C. Busi, A. Papetti, C. Sabelli, D. Lelli, G.L. Alborali, L. Gibelli, D. Gelmetti, A. Lavazza, P. Cordioli, M.B. Boniotti); Università degli Studi di Bari, Bari, Italy (V. Martella)

DOI: <https://doi.org/10.3201/eid2309.170158>

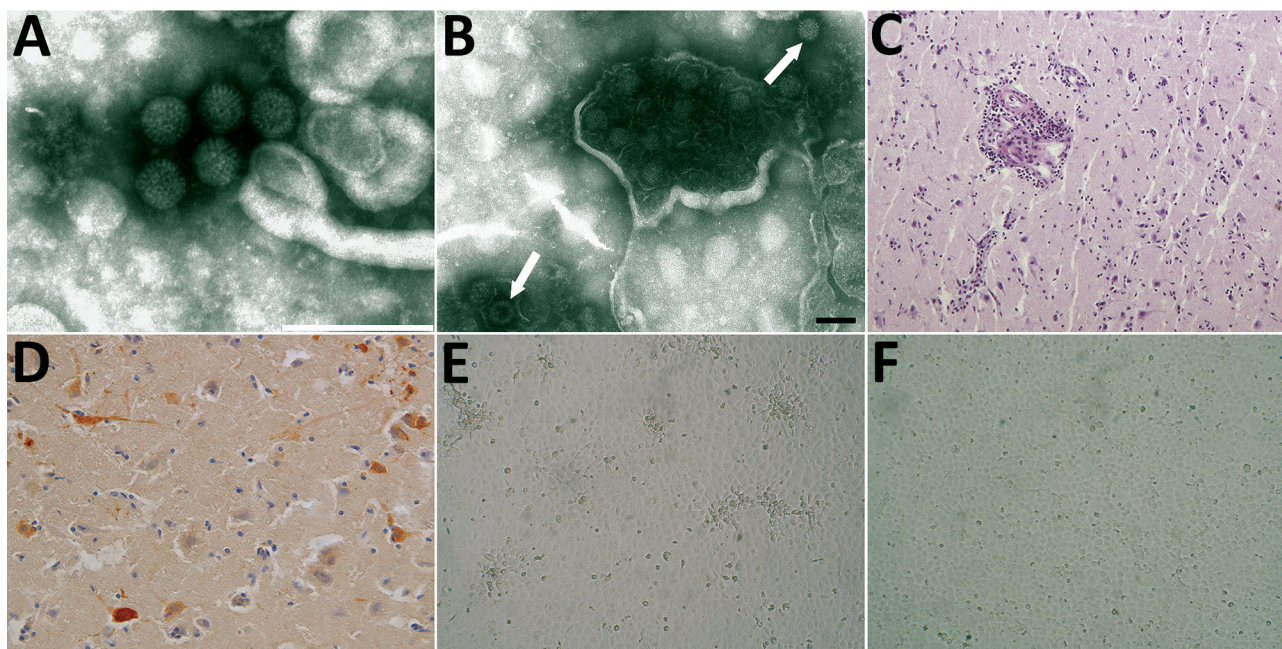


Figure 1. Images of brain of fox with group A rotavirus infection and brains of suckling and weanling mice inoculated with fox brain homogenates. A, B) Negative-staining electron microscopy. Presence of virions morphologically related to family *Reoviridae* from fox (A) and mouse (B) brain (arrows). Scale bar in panel A indicates 200 nm; in panel B, 100 nm. C, D) Histologic and immunohistochemical appearance of the cerebral cortex of the fox. C) Perivascular cuffing of inflammatory cells in the brain stained by hematoxylin and eosin (original magnification $\times 10$). D) Viral antigen in the cytoplasm of neurons (immunohistochemistry, original magnification $\times 20$). E) Foci with rounding cells of the confluent monolayers of Marc-145 cells infected with the brain homogenate from mouse at 2 days after inoculation (original magnification $\times 40$). F) Mock cells (original magnification $\times 40$).

The genome of fox-288356 was 18,849 nt and showed high sequence homology to avian strain PO-13, isolated from a pigeon (2,4). Homology was apparent in most genome segments (89%–94% nt and 91%–98% aa), except for the ninth segment, coding for viral protein (VP) 7 (86% nt and 88% aa), and the tenth segment, coding for nonstructural protein (NSP) 4 (79% nt and 83% aa) (Table 1). After phylogenetic analysis of the concatenated genome (Figure 2) and individual genome segments (online Technical Appendix Figure 3), fox-288356 grouped with avian group A rotaviruses. The genomic constellation of fox-288356 was G18P[17]-R4-C4-M4-A4-I4-T4-N4-E19-H4 (Table 2).

Several amino acid mutations were present in the major antigenic regions (A, B, and C) of VP7 (online Technical Appendix Figure 4) and in key residues of VP4 (online Technical Appendix Figure 5). VP4 contained only 1 of the 3 arginine residues required for trypsin-mediated cleavage into the VP8* and VP5* subunits (10). This finding seems consistent with the ability of fox-288356 to grow in cell cultures in the absence of trypsin, a feature that has been observed for some avian group A rotaviruses (11).

We classified the NSP4 of fox-288356 as a novel E genotype, E19, as indicated by the Rotavirus Classification Working Group. We also found differences between the

Table 1. Comparison of genome segment sizes and sequence similarities among group A rotaviruses isolated from fox and pigeon*

Segment number/encoded protein	Nucleotide/amino acid length (genotype)		% Nucleotide sequence identity	% Amino acid sequence identity
	Fox-288356†	PO-13‡		
1/VP1	3,305/1,089 (R4)	3,302/1,088 (R4)	93	98
2/VP2	2,738/897 (C4)	2,738/897 (C4)	91	97
3/VP3	2,583/829 (M4)	2,583/829 (M4)	91	94
4/VP4	2,349/770 (P[17])	2,349/770 (P[17])	92)	95
5/NSP1	1,871/576 (A4)	1,870/576 (A4)	86	91
6/VP6	1,348/397 (I4)	1,348/397 (I4)	94	98
7/NSP3	1,092/306 (T4)	1,092/306 (T4)	89	95
8/NSP2	1,043/315 (A4)	1,042/315 (N4)	93	95
9/VP7	1,065/329 (G18)	1,065/329 (G18)	86	88
10/NSP4	726/169 (E19)	727/169 (E4)	77	83
11/NSP5	729/218 (H4)	729/218 (H4)	93	90

*NSP, nonstructural protein; VP, viral protein.

†Rotavirus isolated from a red fox.

‡Rotavirus isolated from a pigeon.

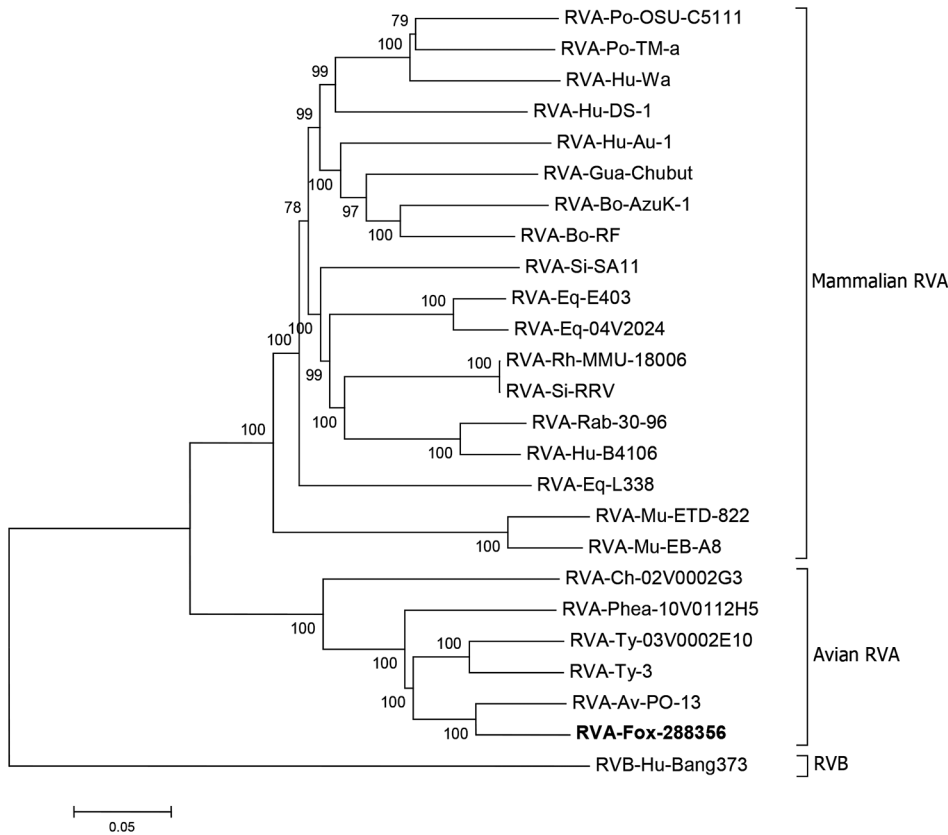


Figure 2. Phylogenetic analysis of RVA strain fox-288356. Analysis was performed on the basis of the concatenated nucleotide sequences of genomic segments. Fox-288356 is correlated with RVA PO-13 (from pigeon) and clustered with the avian RVA. Reference sequences are identified by strain name and GenBank accession number. Scale bar indicates nucleotide substitutions per site. RVA, group A rotavirus; RVB, group B rotavirus.

NSP4 of fox-288356 and other group A rotaviruses (online Technical Appendix Figure 6).

Conclusion

Although in humans group A rotaviruses are mainly associated with gastroenteritis, the literature indicates that group A rotaviruses may also be associated with acute encephalitis or encephalopathy (6–9). This correlation has been supposed for children in whom neurologic signs develop concomitantly or shortly after acute gastroenteritis caused by group A rotavirus (7,9) and after detection of group A rotavirus RNA in the cerebrospinal fluid of patients with neurologic signs (6,8). It remains unclear whether systemic spread of group A rotavirus and localization in the central nervous system is the result of host-related factors, whether it depends on intrinsic

biological features of group A rotavirus strains, or whether it eventually results from a combination of both elements. Fox-288356 was probably responsible for the neurologic disease observed in the fox, as suggested by the results of our diagnostic investigations and by the inflammatory lesions in the brain of the animal.

Genomic characterization indicated that fox-288356 shared the same genetic backbone as avian strain PO-13 and avian-like bovine strain 993-83 (2). Under experimental conditions, oral inoculation of mice with pigeon group A rotavirus strain PO-13 infected and caused diarrhea in the mice, but inoculation with turkey group A rotavirus strain Tyr-1 did not (4). Also, the synthetic NSP4 toxic peptide of strain PO-13 elicited diarrhea in suckling mice (12). It is tempting to speculate that some avian group A rotaviruses (e.g., group A rotaviruses with the PO-13

Table 2. Genomic constellation of avian group A rotavirus strains*

Group A rotavirus strain	VP7	VP4	VP6	VP1	VP2	VP3	NSP1	NSP2	NSP3	NSP4	NSP5
Fox-wt/ITA/288356/2011/G18P[17]	G18	P[17]	I4	R4	C4	M4	A4	N4	T4	E19	H4
Pigeon-tc/JPN/PO-13/1983/G18P[17]	G18	P[17]	I4	R4	C4	M4	A4	N4	T4	E4	H4
Bovine-wt/GER/993_83/1983/G18P[17]	G18	P[17]	I4								
Turkey-tc/GER/03V0002E10/2003/G22P[35]	G22	P[35]	I4	R4	C4	M4	A16	N4	T4	E11	H4
Group A rotavirus/tTurkey-tc/IRL/Ty-3/1979/G7P[35]	G7	P[35]	I4	R4	C4	M4	A16	N4	T4	E11	H14
Group A rotavirus/Turkey-tc/IRL/Ty-1/1979/G17P[38]	G17	P[38]	I4	R4	C4	M4	A16	N4	T4	E4	H4
Pheasant-tc/GER/10V0112H5/2010/G23P[37]	G23	P[37]	I4	R4	C4	M4	A16	N10	T4	E4	H4
Chicken-tc/GER/02V0002G3/2002/G19P[30]	G19	P[30]	I11	R6	C6	M7	A16	N6	T8	E10	H8

*Gray shading indicates homology. NSP, nonstructural protein; VP, viral protein.

genome backbone) have the ability to cross the host-species barrier more easily than other avian group A rotaviruses (Table 1). Another bovine group A rotavirus strain, N2342, with a VP4 gene related to the avian strain PO-13, has been recently identified in Japan (3).

The virus isolated from the fox displayed a unique NSP4, which was proposed as a novel genotype, E19. NSP4 serves as an intracellular receptor for immature particles and interacts with viral capsid proteins during viral morphogenesis (13). NSP4 also acts as a viral enterotoxin (13,14), and the enterotoxic activity has been mapped to a region, the toxic peptide, spanning amino acids 114–135 of NSP4 (14). Changes in residues within the NSP4 toxic peptide have been associated with alterations in the toxigenic activity of NSP4 and in rotavirus virulence (15).

The detection of fox-288356 in the brain of a fox supports the accumulating clinical evidence for the association between group A rotaviruses and neurologic signs in human patients. Whether some group A rotavirus strains intrinsically possess the ability to spread to the central nervous system, thereby causing neurologic disease, remains to be explored.

Acknowledgments

We thank Chiara Garbarino, Anna Tirelli, and Giuseppe Bertocchi for their technical support and Krisztian Banyai for his critical revision of the manuscript.

Dr. Busi is a scientist at the Istituto Zooprofilattico Sperimentale della Lombardia e Emilia Romagna. Her primary research interests include molecular diagnosis and epidemiology of viral and bacterial infectious diseases.

References

- Martella V, Bányai K, Matthijnssens J, Buonavoglia C, Ciarlet M. Zoonotic aspects of rotaviruses. *Vet Microbiol*. 2010;140:246–55. <http://dx.doi.org/10.1016/j.vetmic.2009.08.028>
- Rohwedder A, Schütz KI, Minamoto N, Brüssow H. Sequence analysis of pigeon, turkey, and chicken rotavirus VP8* identifies rotavirus 993/83, isolated from calf feces, as a pigeon rotavirus. *Virology*. 1995;210:231–5. <http://dx.doi.org/10.1006/viro.1995.1338>
- Mitake H, Ito N, Okadera K, Okada K, Nakagawa K, Tanaka T, et al. Detection of avian-like rotavirus A VP4 from a calf in Japan. *J Vet Med Sci*. 2015;77:221–4. <http://dx.doi.org/10.1292/jvms.14-0379>
- Mori Y, Sugiyama M, Takayama M, Atoji Y, Masegi T, Minamoto N. Avian-to-mammal transmission of an avian rotavirus: analysis of its pathogenicity in a heterologous mouse model. *Virology*. 2001;288:63–70. <http://dx.doi.org/10.1006/viro.2001.1051>
- Uhnnoo I, Riepenhoff-Talty M, Dharakul T, Chegas P, Fisher JE, Greenberg HB, et al. Extramucosal spread and development of hepatitis in immunodeficient and normal mice infected with rhesus rotavirus. *J Virol*. 1990;64:361–8.
- Dickey M, Jamison L, Michaud L, Care M, Bernstein DI, Staat MA. Rotavirus meningoencephalitis in a previously healthy child and a review of the literature. *Pediatr Infect Dis J*. 2009;28:318–21. <http://dx.doi.org/10.1097/INF.0b013e31818d8bbe9>
- Kobayashi S, Negishi Y, Ando N, Ito T, Nakano M, Togari H, et al. Two patients with acute rotavirus encephalitis associated with cerebellar signs and symptoms. *Eur J Pediatr*. 2010;169:1287–91. <http://dx.doi.org/10.1007/s00431-010-1202-y>
- Arakawa C, Fujita Y, Imai Y, Ishii W, Kohira R, Fuchigami T, et al. Detection of group A rotavirus RNA and antigens in serum and cerebrospinal fluid from two children with clinically mild encephalopathy with a reversible splenic lesion. *Jpn J Infect Dis*. 2011;64:204–7.
- Rath BA, Gentsch J, Seckinger J, Ward K, Deputy S. Rotavirus encephalitis with basal ganglia involvement in an 8-month-old infant. *Clin Pediatr (Phila)*. 2013;52:260–4. <http://dx.doi.org/10.1177/0009922811417301>
- Trask SD, Wetzel JD, Dermody TS, Patton JT. Mutations in the rotavirus spike protein VP4 reduce trypsin sensitivity but not viral spread. *J Gen Virol*. 2013;94:1296–300. [10.1099/vir.0.050674-0](http://dx.doi.org/10.1099/vir.0.050674-0) <http://dx.doi.org/10.1099/vir.0.050674-0>
- McNulty MS, Allan GM, Todd D, McFerran JB, McKillop ER, Collins DS, et al. Isolation of rotaviruses from turkeys and chickens: demonstration of distinct serotypes and RNA electrophoretotypes. *Avian Pathol*. 1980;9:363–75. <http://dx.doi.org/10.1080/03079458008418420>
- Mori Y, Borgan MA, Ito N, Sugiyama M, Minamoto N. Diarrhea-inducing activity of avian rotavirus NSP4 glycoproteins, which differ greatly from mammalian rotavirus NSP4 glycoproteins in deduced amino acid sequence in suckling mice. *J Virol*. 2002;76:5829–34. <http://dx.doi.org/10.1128/JVI.76.11.5829-5834.2002>
- Ramig RF. Pathogenesis of intestinal and systemic rotavirus infection. *J Virol*. 2004;78:10213–20. <http://dx.doi.org/10.1128/JVI.78.19.10213-10220.2004>
- Lorrot M, Vasseur M. How do the rotavirus NSP4 and bacterial enterotoxins lead differently to diarrhea? *Virology*. 2007;4:31. <http://dx.doi.org/10.1186/1743-422X-4-31>
- Zhang M, Zeng CQ, Dong Y, Ball JM, Saif LJ, Morris AP, et al. Mutations in rotavirus nonstructural glycoprotein NSP4 are associated with altered virus virulence. *J Virol*. 1998;72:3666–72.

Address for correspondence: M. Beatrice Boniotti, Research and Development Laboratory, Istituto Zooprofilattico Sperimentale della Lombardia e Emilia Romagna, via Bianchi 9, 25124 Brescia (BS), Italy; email: mariabeatrice.boniotti@izsler.it

Group A Rotavirus Associated with Encephalitis in Red Fox

Technical Appendix

Additional Methods and Details

Viruses

During a national surveillance program for rabies in wildlife animals, a red fox (*Vulpes vulpes*) was captured in the Apennines of Piacenza province, Italy. The animal showed nervous disorders, including ataxia and head shaking. Due to bad general conditions, the fox was euthanized and the brain of the animal was collected and screened for a panel of neuro-pathogens, as requested by the Italian veterinarian health system.

Screening for neuro-pathogens

The animal was tested with a diagnostic panel specific for neuro-pathogens: rabies, canine distemper, Aujeszky's disease, leishmaniasis and flavivirus infections. Mouse inoculation test and Fluorescent Antibody Test (FAT) for rabies virus were performed according to the OIE guidelines (OIE 2013). Briefly, ten Specific Pathogen-Free (SPF) Swiss mice of 2 days of age (“suckling mice”) and ten 17-day old mice (“weaning mice”) were inoculated intracerebrally with 30 μ L of clarified supernatant obtained from a 10% (w/v) homogenate of brain material made in an isotonic buffered solution containing antibiotics. Three mice were used as controls. The mice were observed daily, and each dead mouse was examined for rabies using the FAT assay. Detection of canine distemper virus, Aujeszky's disease virus, flavivirus and *Leishmania infantum* was performed by Reverse transcriptase-PCR (RT-PCR) or PCR as previously described (1–4).

Electron Microscopy (EM)

The brain homogenates of the naturally infected fox and the experimentally infected mice were submitted to negative staining electron microscopy using the Airfuge method (5). Viral particles were spun directly onto grids in an ultracentrifuge (82,000 x g, 15 min; Airfuge® with

fixed-angle rotor A-100/18 (Beckman Coulter, USA, California, Brea) and contrasted with phosphotungstic acid (PTA). The morphological identification of viral particles was obtained by observation with a FEI (Eindhoven, NL) Tecnai G2 Spirit Biotwin electron microscope at different magnifications (range, 20,500x to 43,000x).

Histology and immunohistochemistry (IHC)

A fragment of frozen cerebrum was fixed in 10% buffered formalin, paraffin-embedded and cut into serial sections of 3 μm thickness. A section was stained with hematoxylin-eosin (HE), whilst the other sections were incubated overnight with a polyclonal serum raised against RVA (IZSLER, Italy, Brescia), diluted 1:2000 and developed with Novolink™ polymer detection system (Leica, Germany, Wetzlar), using Vector® NovaRED™ substrate kit as chromogen.

Culture isolation, virus purification, RNA extraction, and electropherotype

Homogenate of the fox brain was used to infect confluent monolayers of Marc-145 cells (a highly homogenous MA-104 derived cell line) in Minimum Essential Medium (MEM), without and with 10 $\mu\text{g}/\text{mL}$ trypsin.

Homogenates from the fox cerebral tissues, from the brain of mice infected with the fox homogenate and from Marc-145 infected cells, were purified by centrifugation at 35,000 $\times g$ for 2 h on a 24% sucrose layer at 4°C in an SW40 rotor (Beckman Coulter, USA, California, Brea). The pellets were suspended in 200 μL of MEM. Subsequently, the samples were treated with distilled water (1:1, v/v), for 15 min at room temperature to remove residual host cells. Non-encapsidated DNA was removed by digestion with 10 U of DNase I (Invitrogen, USA, California, Carlsbad), at 65°C for 10 minutes with 50 μl of 10X DNase I reaction buffer (Invitrogen).

Viral RNA was extracted using EuroGold RNA Pure solution (Euroclone, Italy, Milan) according to manufacturer's protocol. Purified viral RNA was quantified spectrophotometrically (NanoQuant, Tecan) and stored at -20°C.

Electrophoresis of the extracted RNA was carried out in 7.5% polyacrylamide slab gels with a 3.5% stacking gel, using the discontinuous buffer system described by Laemmli (1970) (6) without sodium dodecyl sulfate. Electrophoresis was performed at 100 V for 16 to 18 h at

4°C. SilverXpress® Silver Staining Kit (Invitrogen), was applied to visualize RNA segments according to manufacturer's protocol.

Genome sequencing

Sequence-independent amplification of viral nucleic acids was performed, as previously described by Victoria JG et al. 2008 (7), by incubation of the extracted viral RNA with 5 pmol of primer K-8N (GAC CAT CTA GCG ACC TCC ACN NNN NNN N), and 0.5 mM of each deoxynucleoside triphosphate (dNTP) at 75°C for 5 min. Subsequently, 5U of RNase inhibitor, 10 mM dithiothreitol, 1X first-strand buffer, and 200 U of SuperScript® II reverse transcriptase (Invitrogen) were added to the mixture and incubated at 25°C for 5 min, followed by an incubation at 37°C for 1 hr. A single round of double-strand (ds) DNA synthesis was then performed using Klenow fragment polymerase (New England Biolabs, USA, Massachusetts, Ipswich): 20 µl of cDNA were heated at 95°C for 2 min and then cooled at 4°C in the presence of 0,5 pmol of primer K-8N and 1X NEB buffer, 0,125 U of DNA polymerase I, large (klenow) fragment. Reaction was performed at 37°C for 60 min. Finally, the reaction products were purified by NucleoSpin® gel and PCR clean-up (Macherey-Nagel, Germany, Düren) following manufacturer's procedure. PCR amplification of nucleic acids was then performed using primer K (GAC CAT CTA GCG ACC TCC AC), consisting of the fixed portion of the random primers K-8N. Five µl of the reaction described above was used in a total reaction volume of 25 µl containing 0,2 mM of each dNTP, 1X GoTaq® Reaction buffer, 0,8 pmol of primer K, and 0,1 U of GoTaq® DNA polymerase (Promega, USA, Wisconsin, Madison). Temperature cycling was performed as follows: 1 cycle at 95°C for 3 min, 25 cycles of denaturing at 95°C for 30 sec, annealing at 55°C for 30 sec, extension at 72°C for 1 min. An additional extension step at 72°C for 7 min was added to the end of the run. PCR was loaded on a 2% agarose gel electrophoresis where a smear of fragments was observed. Fragments larger than 500bp were purified by Nucleospin® gel and PCR clean-up (Macherey-Nagel) and used for subcloning into pCR™ 2.1 vector (Invitrogen) according to manufacturer's instruction.

Thirty-seven clones were sequenced using M13 primers. The sequences obtained from the clones covered around 14.6% of the genome (Figure 2 online Technical Appendix). The remaining genome sequences were obtained by amplification with specific primers. The primers were designed using the alignment of the sequences obtained from the clones and the genome sequence of the avian RVA strain PO-13 (online Technical Appendix Table 1). Reverse

transcription was performed using 1 µg of RNA with 10 pmol of random primers and 10 mM of each dNTP, heating at 65°C for 5 min followed by rapid cooling on ice. Then, 10 mM dithiothreitol and 1X first-strand buffer were added to the mixture and incubated at 25°C for 2 min. Subsequently, 200 U of SuperScript™ II reverse transcriptase (Invitrogen) was added to the 20-µL final mixture and then incubated at 25°C for 10 min and then at 42°C for 50 min and terminated at 70°C for 15 min. The PCR assays were performed in a Veriti Thermal Cycler (Applied Biosystems, USA, California, Foster City) using 1 µL of cDNA in a total reaction volume of 25 µL containing 0.2 mM of each dNTP, 1X GoTaq® reaction buffer, 1 pmol primer, and 0.1 U of GoTaq® DNA polymerase (Promega). Thermal cycling was performed as follows: 1 cycle at 95°C for 3 min, 35 cycles of denaturation at 95°C for 30 sec, annealing at 46-50°C for 30 sec and extension at 72°C for 1 min, and a final extension step at 72°C for 7 min. The PCR products were purified with the Nucleospin® gel and PCR clean-up Kit (Macherey-Nagel). Sequencing reactions were performed with fluorescent dideoxy chain-termination chemistry using the BigDye® Terminator v1.1 cycle sequencing kit (Applied Biosystems) on an automated sequencer (ABI PRISM® 3130 Automated Capillary DNA Sequencer, Applied Biosystems).

Finally, the 3'- and 5'-terminal sequences of the genome segments were determined by a primer ligation strategy (8), with minor modifications. Briefly, extracted RNA was ligated with a single amino-linked modified oligonucleotide (Linker: 5'-PO₄-TTC CTT ATG CAG CTG ATC ACT CTG TGT CA-C₆-NH₂-3') to the 3'-end of both strands of dsRNA. About 1 µg of viral RNA was added to 8 µL of 10X T4 RNA Ligase buffer (Promega), 40 µL of 40% PEG 8000, 2 µL OligoLinker (final concentration ≈ 1 µM), 20 U T4 RNA Ligase (Promega) in a final volume of 83 µL, incubated at room temperature for 2 hours and then stored at -20°C. Five µL of ligation product was used as template for a One-Step RT-PCR (Qiagen, Germany, Hilden) reaction with a first primer chosen inside the sequence of the virus (Online Technical Appendix Table 2) and the second primer complementary to the linker sequence (5'-TGA CAC AGA GTG ATC AGC-3'). Thermal cycling was performed as follows: reverse transcription at 45°C for 30 min, enzyme activation at 95°C for 15 min, gradual cooling down from 83°C to 65°C, 3 min for step (8 step), 45 cycles of denaturing at 94°C for 30 sec, annealing at 46-50°C for 30 sec and extension at 72°C for 1 min. A final extension step at 72°C for 10 min was added to the end of the run.

Sequence analysis

The sequences obtained were assembled and aligned using the SeqMan module of the DNASTAR software package (Lasergene, USA, Madison). Genotype assignment of each segment was performed using the RotaC v2.0 (<http://rotac.regatools.be>) automated genotyping tool for RVAs. The assignment of the novel NSP4 genotype was approved by the Rotavirus Classification Working Group (RCWG). (<https://rega.kuleuven.be/cev/viralmetagenomics/virus-classification/rcwg>). The sequences of the genomic segments of RVA/Fox-wt/ITA/288356/2011 have been deposited in GenBank under accession numbers KT873803 through KT873813. Phylogenetic analysis was performed on both concatenated and separate nucleotide sequences obtained from the genomic segments using the Neighbor-Joining method p-distance model and bootstrap test of 1,000 replicates in MEGA 5 (<http://www.megasoftware.net/>).

References

1. Frisk AL, König M, Moritz A, Baumgärtner W. Detection of canine distemper virus nucleoprotein RNA by reverse transcription-PCR using serum, whole blood, and cerebrospinal fluid from dogs with distemper. *J Clin Microbiol.* 1999;37:3634–43.
2. Yoon HA, Eo SK, Aleyas AG, Park SO, Lee JH, Chae JS, et al. Molecular survey of latent pseudorabies virus infection in nervous tissues of slaughtered pigs by nested and real-time PCR. *J Microbiol.* 2005;43:430–6.
3. Scaramozzino N, Crance JM, Jouan A, DeBriel DA, Stoll F, Garin D. Comparison of flavivirus universal primer pairs and development of a rapid, highly sensitive heminested reverse transcription-PCR assay for detection of flaviviruses targeted to a conserved region of the NS5 gene sequences. *J Clin Microbiol.* 2001;39:1922–7. <http://dx.doi.org/10.1128/JCM.39.5.1922-1927.2001>
4. Galletti E, Bonilauri P, Bardasi L, Fontana MC, Ramini M, Renzi M, et al. Development of a minor groove binding probe based real-time PCR for the diagnosis and quantification of *Leishmania infantum* in dog specimens. *Res Vet Sci.* 2011;91:243–5. <http://dx.doi.org/10.1016/j.rvsc.2011.01.004>
5. Lavazza A, Pascucci S, Gelmetti D. Rod-shaped virus-like particles in intestinal contents of three avian species. *Vet Rec.* 1990;126:581.

6. Laemmli UK. Cleavage of structural proteins during the assembly of the head of bacteriophage T4. *Nature*. 1970;227:680–5. <http://dx.doi.org/10.1038/227680a0>
7. Victoria JG, Kapoor A, Dupuis K, Schnurr DP, Delwart EL. Rapid identification of known and new RNA viruses from animal tissues. *PLoS Pathog*. 2008;4:e1000163. <http://dx.doi.org/10.1371/journal.ppat.1000163>
8. Matthijnssens J, Rahman M, Van Ranst M. Two out of the 11 genes of an unusual human G6P[6] rotavirus isolate are of bovine origin. *J Gen Virol*. 2008;89:2630–5. <http://dx.doi.org/10.1099/vir.0.2008/003780-0>
9. Zhang M, Zeng CQ, Dong Y, Ball JM, Saif LJ, Morris AP, et al. Mutations in rotavirus nonstructural glycoprotein NSP4 are associated with altered virus virulence. *J Virol*. 1998;72:3666–72.
10. Mohan KV, Dermody TS, Atreya CD. Mutations selected in rotavirus enterotoxin NSP4 depend on the context of its expression. *Virology*. 2000;275:125–32. <http://dx.doi.org/10.1006/viro.2000.0484>
11. Jagannath MR, Kesavulu MM, Deepa R, Sastri PN, Kumar SS, Suguna K, et al. N- and C-terminal cooperation in rotavirus enterotoxin: novel mechanism of modulation of the properties of a multifunctional protein by a structurally and functionally overlapping conformational domain. *J Virol*. 2006;80:412–25. <http://dx.doi.org/10.1128/JVI.80.1.412-425.2006>

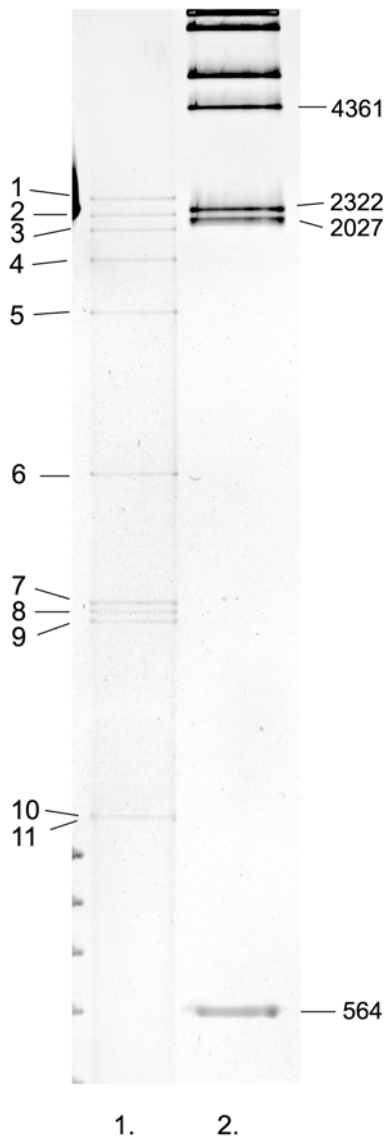
Technical Appendix Table 1. Primers used for amplification and sequencing of the genome segments of the strain RVA/Fox-wt/ITA/288356/2011

Segment number (encoded protein)	Name	Sequence (5' → 3')	position (nt)	Amplicon size
1 (VP1)	VP1_9F	GGCTATTAAGCTATACGATG	1 - 21	740
	VP1_18R	AGTTGATCTGTTCGAATATG	740 - 721	
	VP1_11F	TAAC TTGGGCAAATTCATCA	629 - 648	330
	VP1_12R	GGTGCATCTATCCAGTTCCTT	959 - 939	
	VP1_2F	CACAACGGAAGAACTTGAAC	854 - 817	385
	VP1_3R	TTGTCTGGACTCACCATTCCG	1239 - 1220	
	VP1_13F	GTTGATTCAGAACTAGCTGG	1180 - 1199	516
	VP1_14R	CGAGTGTTCCTTAACTTTCCCT	1696 - 1675	
	VP1_15F	ATACTGACGTATCGCAATGG	1574 - 1593	804
	VP1_16R	CGCTGTAATACACATCGTC	2378 - 2359	
	VP1_8F	G TACTGACTACGAACTCAACG	2284 - 2304	1016
	VP1_10F	TCATATCTTAGCGCCTTAATC	3300 - 3280	
2 (VP2)	VP2_20F	AGAAGGAGGTGCAATATGAA	316 - 335	275
	VP2_21R	CGAGTACTTGCGAATAAAGG	591 - 572	
	VP2_2F	TGGATGGTATTGGAAATTG	500 - 518	695
	VP2_5R	TTCGCTGCTTGAGAGTTAAT	1195 - 1176	
	VP2-10F	TCGAGTCAATCTGGGATGCT	1009 - 1028	491
	VP2-11R	TGTGGTTGACAAAATGTAGC	1500 - 1481	
	VP2-16F	CAAAACGATCATAGCGTGTA	1205 - 1224	765
	VP2_7R	ATACAGGTCCAGATGGTTTG	1970 - 1951	
	VP2_12F	AGAGCCACGTACACTGTTTC	1853 - 1872	885
		VP2_9R	GGTCATATCACCATTTACG	2738 - 2720
3 (VP3)	VP3_5F	GGCTATTAAGCTACATGAG	1 - 20	659
	VP3_1R	TAGTGTCTTTTGGCACCTTC	659 - 640	
	VP3_2F	TCAGATAGAAATGGCGTTG	1067 - 1085	944
	VP3_3R	TGCATATAGCAATTCTGGTG	2011 - 1992	
4 (VP4)	VP4_5F	GGCTATAAATGGCTTCTC	1 - 19	769
	VP4_4R	TTGAAATCACTATGTCTTCG	769 - 750	
	VP4_11F	ATGCCAGTTGAACGATTAGT	703 - 722	470
	VP4_12R	TCCAAGTGGAAAGTTGAAAAT	1173 - 1154	
	VP4_8F	AGGCATTCAAAAACATGGTA	1076 - 1095	520
	VP4_1R	TCCAGAAAACATTGAGAAC	1596 - 1578	
	VP4_13F	GGAAATAGCAATGTCTCAGC	1527 - 1546	389
	VP4_14R	TTTAATACAGCAGCCGAAAT	1916 - 1896	
	VP4_2F	AGAGTGAAAGAAATTCGCAAC	1846 - 1865	503
	VP4_6R	GGTCACATCCTCATAGAC	2349 - 2332	
5 (NSP1)	NSP1_5R	GGCTTTTAAAGCTGAACAG	1 - 20	661
	NSP1_1R	CTCTGAGGCTCATAATGTCCA	661 - 641	
	NSP1_9F	ATTGTTTCCTGCCAACAAAT	550 - 569	606
	NSP1_10R	ATGTCTTCCAAATTGTCCAG	1156 - 1137	
	NSP1_4F	GGATGGACTCACTTCTCATAC	1092 - 1112	778
	NSP1_6R	GGTCTCATAAAGCCATTTTG	1870 - 1851	
6 (VP6)	VP6_7F	CTGATTCGCTAAGACAGCTT	361 - 381	690
	VP6_8R	AATATGGCTCATTTGCATCT	1051 - 1031	
7 (NSP3)	NSP3_5R	GGCTTTTAAAGTCACATCGAG	1 - 21	526
	NSP3_7R	ATCACTTCCCCACGTTTGAG	526 - 506	
	NSP3_9F	AGGATGATGCTTTCTGCTAA	381 - 400	711
	NSP3_6R	GGTCACATAAAGTCTCGTGC	1092 - 1073	
8 (VP7)	VP7_3F	GGCATTAAAATCAGTAATTTTC	1 - 22	189
	VP7_1R	GCGGCAAAAACAATAGTAAG	189 - 170	
	VP7_2F	GACACGCATTAATTGGAAG	910 - 928	155
	VP7_4R	GGTCACATCAATCCTTCAC	1065 - 1047	
9 (NSP2)	NSP2_3R	GGCTTTTAAAGCGTCTCGG	1 - 19	889
	NSP2_1R	CTAGTTTCATCCCATTACGC	889 - 870	
	NSP2_2F	ACCATTTAAAGGAGTCAGC	935 - 954	107
	NSP2_4R	GGTCACATAAAGCGCTTTCAATTC	1042 - 1019	
10 (NSP4)	NSP4_3F	GGAAAGATGGAGAACGCTAC	35 - 54	257
	NSP4_6R	GAGACCACTTCAGTTTTTGAG	292 - 312	
	NSP4_7F	GGATTTAAAGTAGTGGGGGT	230 - 249	444

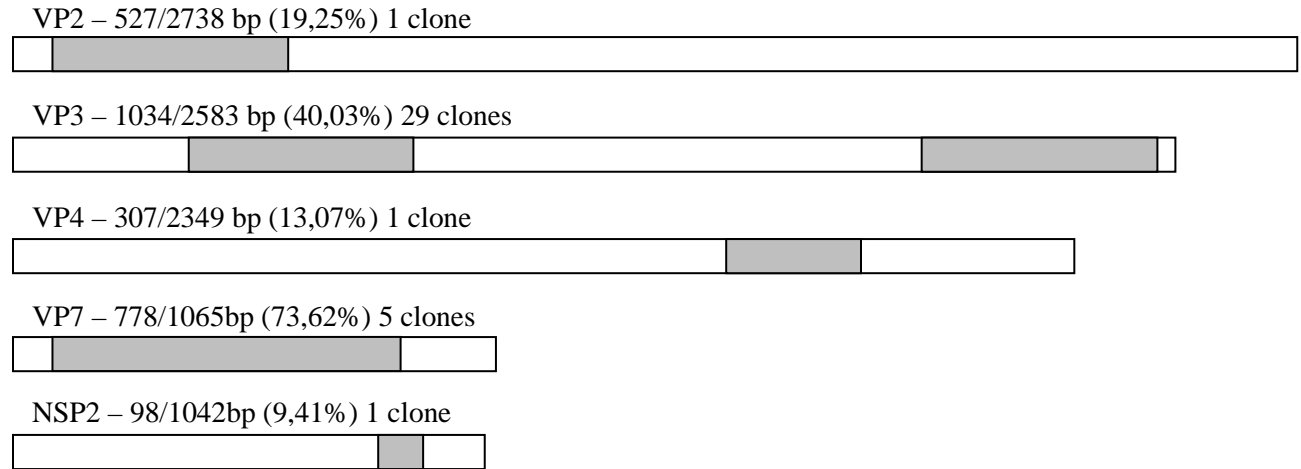
Segment number (encoded protein)	Name	Sequence (5' → 3')	position (nt)	Amplicon size
	NSP4_4R	GGTACCAGGGATTAAGTCTTC	674 - 654	
11 (NSP5)	NSP5_2F	GGCTTTTAAAGCGCTACAGTG	1 - 21	311
	NSP5_5R	TCTGCTGAGCTAGCATCAA	311 - 292	

Technical Appendix Table 2. Primers used for the determination of the 5' and 3' terminal sequences

Segment number (encoded protein)	Name	Sequence (5'-3')	position (nt)
1 (VP1)	VP1_19R	CAACTGTGGCATATTCCTTT	304 - 285
	VP1_20F	TAATGCTACTCGGTGTACCA	2906 - 2925
2 (VP2)	VP2_19R	GTCTCGTTAGGTTGAAATGA	376 - 358
	VP2_15F	ACTGGACGCTACAGTCTTTG	2399 - 2418
3 (VP3)	VP3_7F	CAGGCAAATGTATTCTTCA	410 - 391
	VP3_8F	GCATTAATTTATTAACTCAATACACA	2276 - 1302
4 (VP4)	VP4_9R	AGCATATTTCTTATTCGTTGC	318 - 298
	VP4_10F	CCAACGCGTCAGTATAGAAT	1996 - 2015
5 (NSP1)	NSP1_11R	CACAAGCAAAAACATTATGG	261 - 242
	NSP1_12F	CACAAGAAATGAGAAGAAAA	1576 - 1596
6 (VP6)	VP6_9R	CTCACGCACTATCTCATCAA	333 - 614
	VP6_10F	CAGTTCTGTGAGATGCAAAT	1022 - 1041
7 (NSP3)	NSP3_11R	GATTCAGTACGCCATTCT	315 - 297
	NSP3_12F	GGAATGGAAATTCAACTCAA	791 - 810
8 (VP7)	VP7_5R	AATGCATAGACTAGAGACTAAACC	317 - 284
	VP7_6F	CAATTATTCAGTCGCATCG	769 - 787
9 (NSP2)	NSP2_6R	AAAGTTCATCCCTCTGGAAT	258 - 239
	NSP2_7F	CAATCCAAAAGAGAAATCCA	782 - 801
10 (NSP4)	NSP4_8R	GAGCCAAATGTCTTCTTATACA	293 - 271
	NSP4_9F	ACAAAACGGGAACTAGAACA	388 - 407
11 (NSP5)	NSP5_5R	TCTGCTGAGCTAGCATCAA	311 - 292
	NSP5_6F	GGCTCATCAGCTAAATTAACA	441 - 462



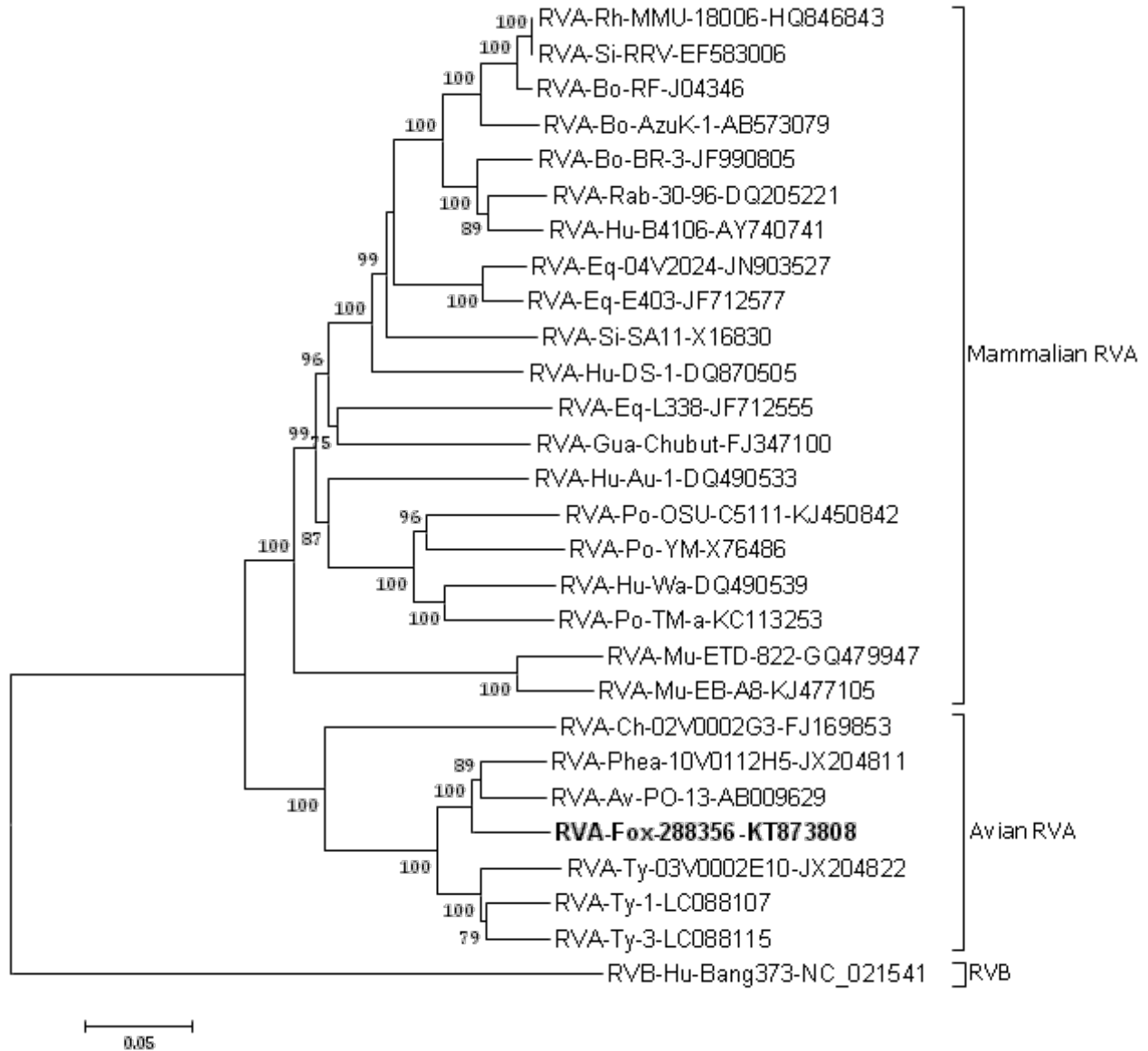
Technical Appendix Figure 1. Electrophoretic migration pattern of genomic RNA segments from the strain Fox-288356 amplified on culture cells on 7,5% polyacrylamide gel (lane 1). The segmented viral genome was characterized by a 5-1-3-2 profile with co-migration of segment 10 and 11. Gene segments are numbered on the left. The molecular marker was load on lane 2.



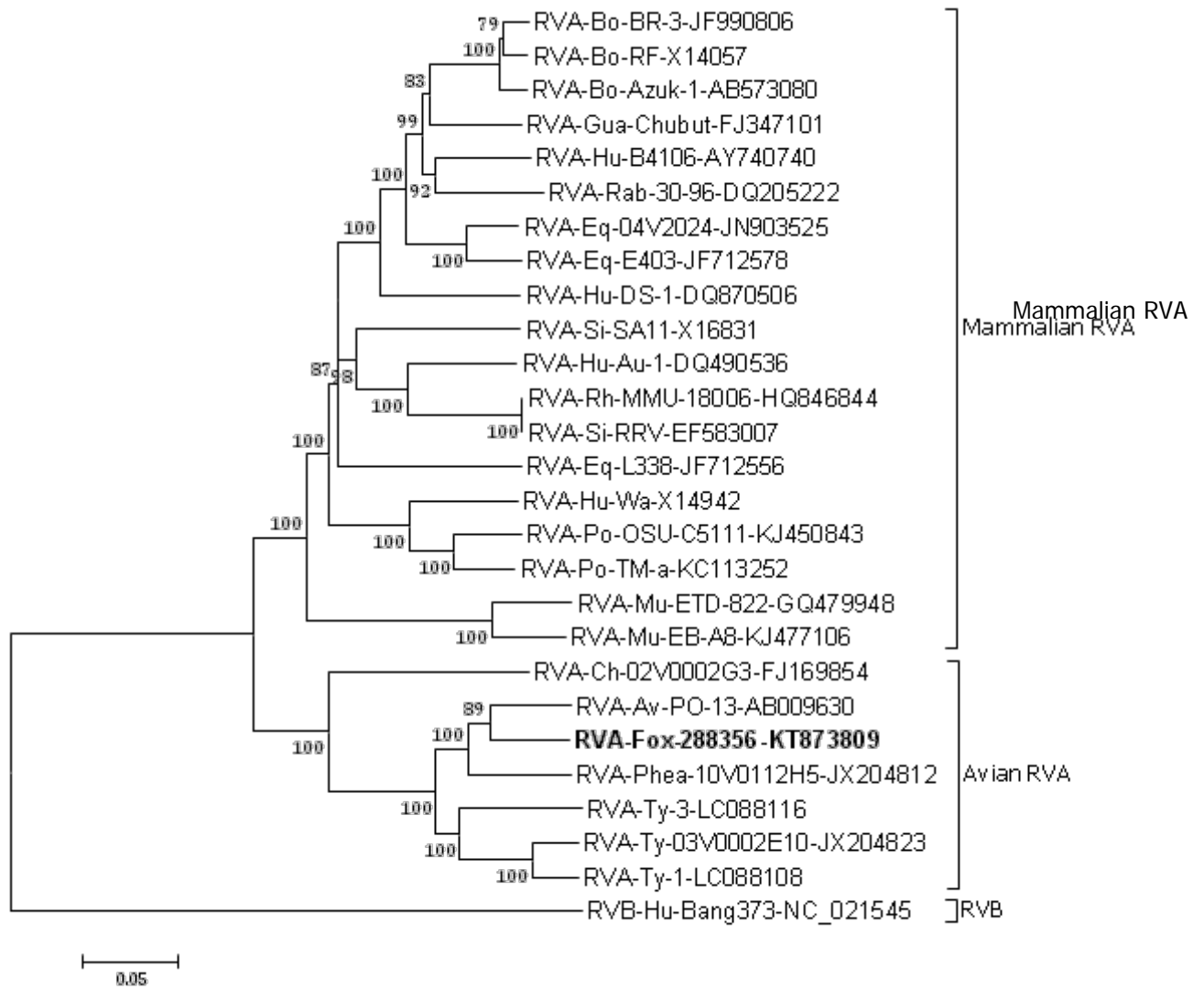
Technical Appendix Figure 2. Schematic representation of the clones obtained by the SISPA method.

Technical Appendix Figure 3 (following pages). Phylogenetic analysis of the genomic segments of the Fox-288356 strain. VP1 (A), VP2 (B), VP3 (C), VP4 (D), VP6 (E), VP7 (F), NSP1 (G), NSP2 (H), NSP3 (I), NSP4 (J), NSP5 (K). All the genomic segments are correlated to the strain RVA-PO-13 and clustered with the avian RVA. Bootstrap values >70% (1,000 replicates) are indicated. Reference sequences are identified by strain name and GenBank accession no.

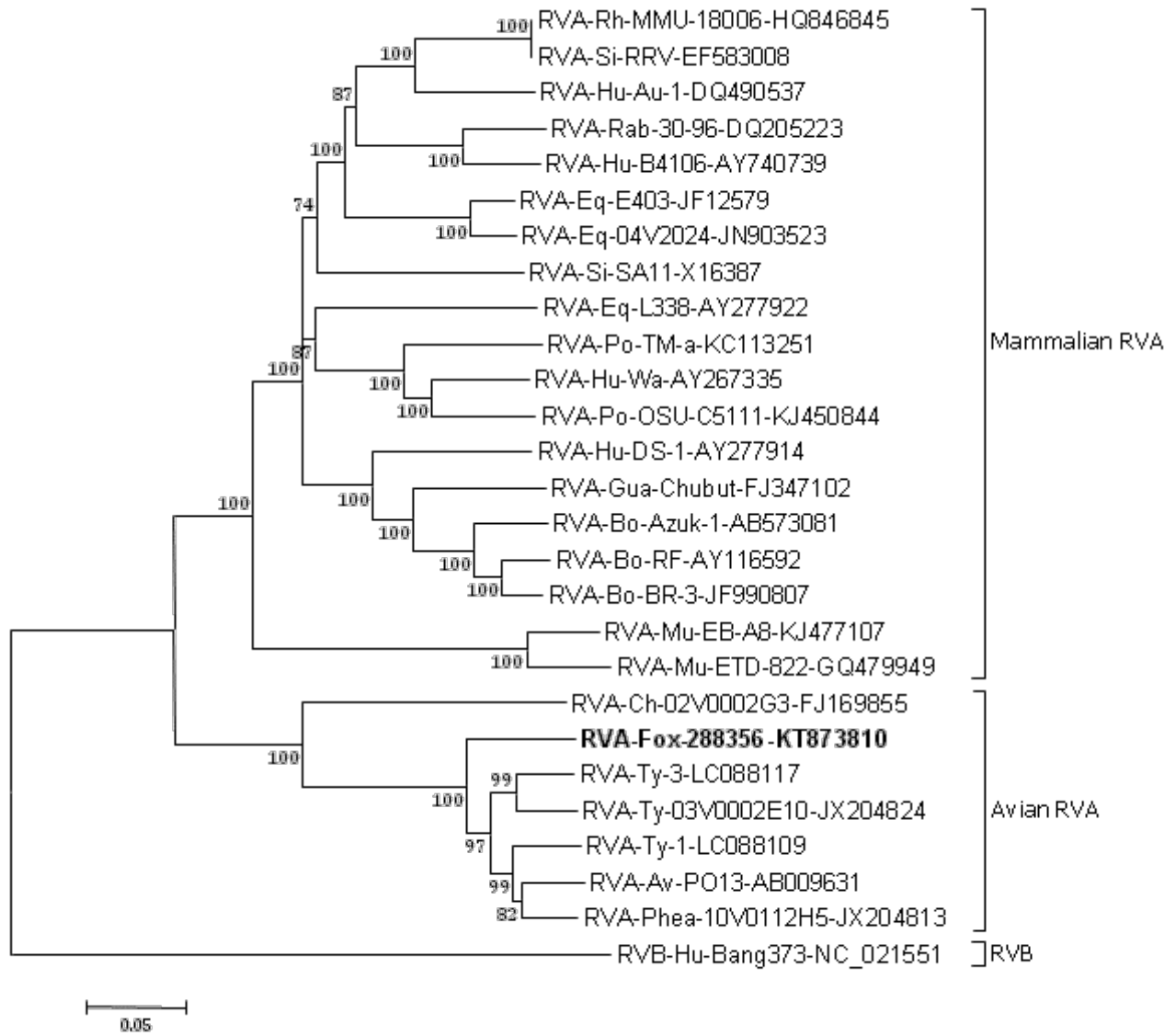
(A) VP1



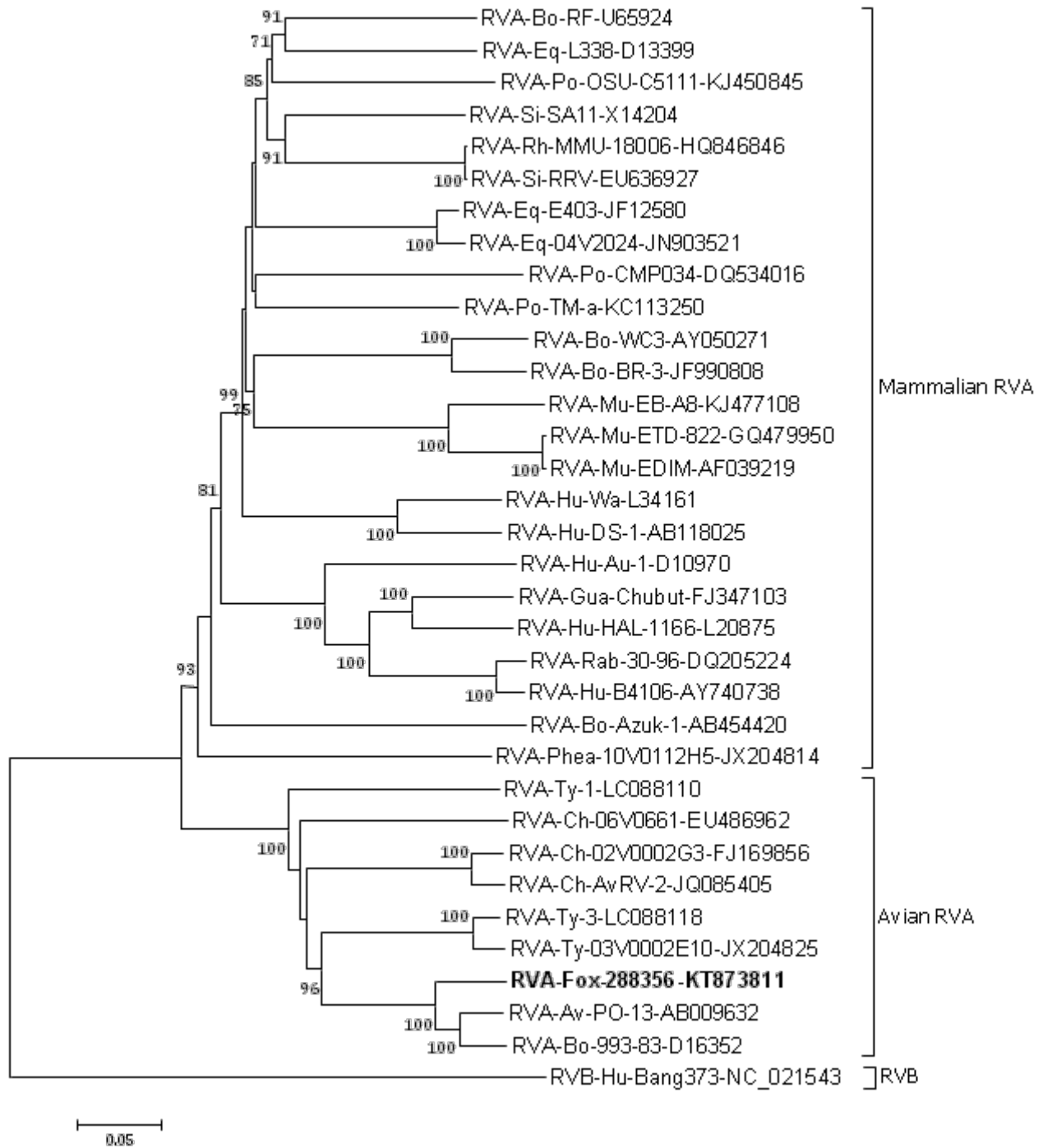
(B) VP2



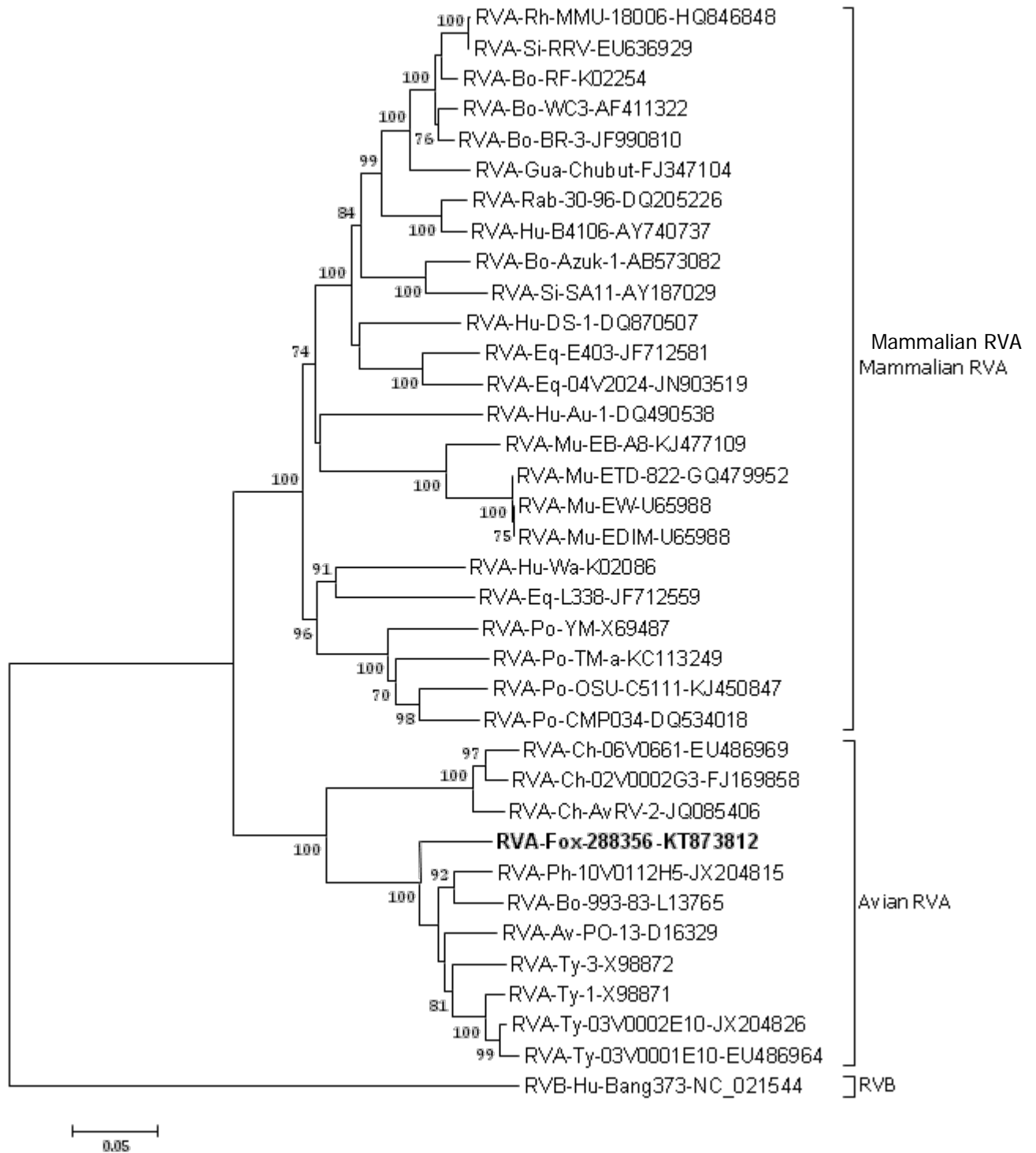
(C) VP3



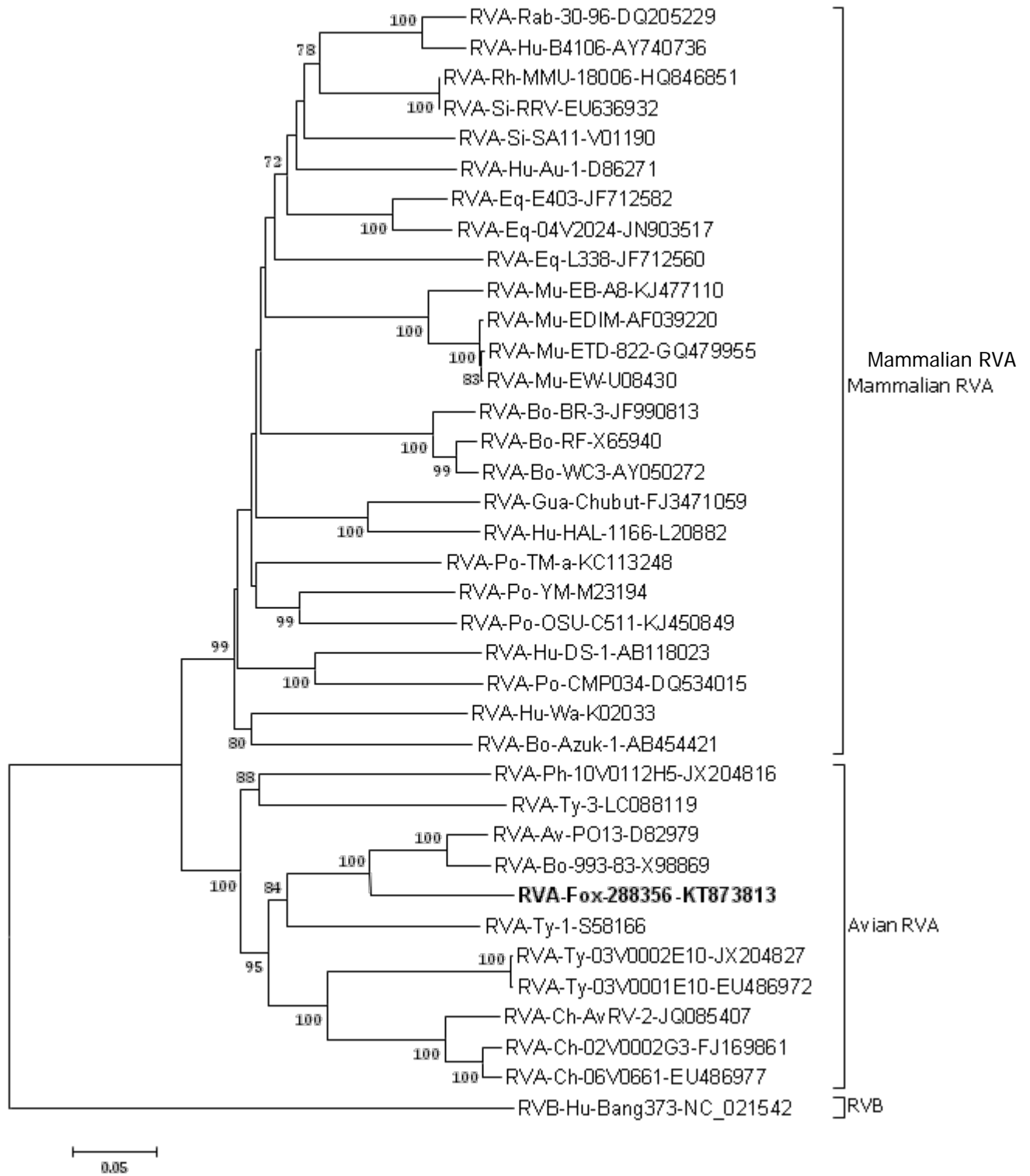
(D) VP4



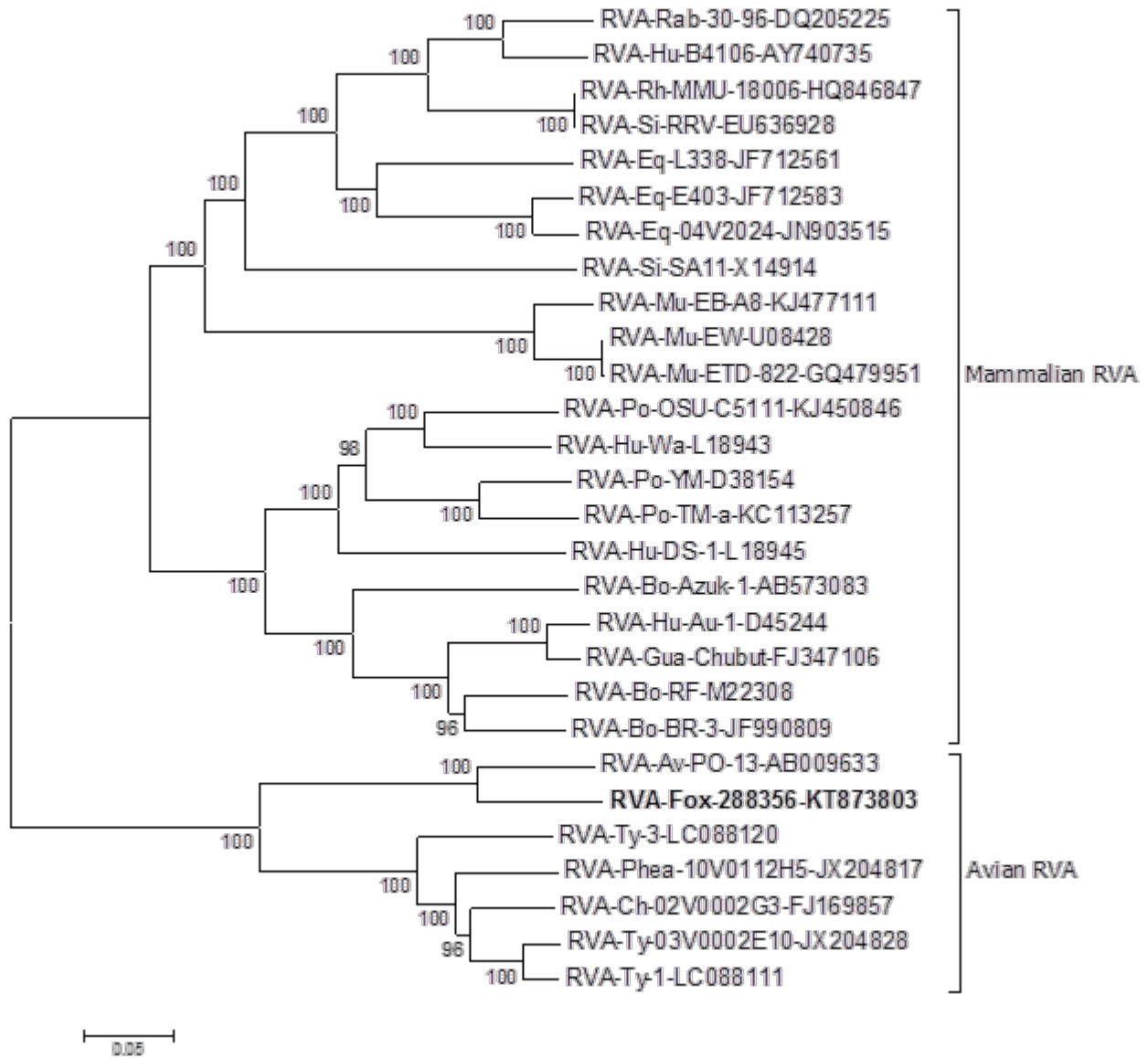
(E) VP6



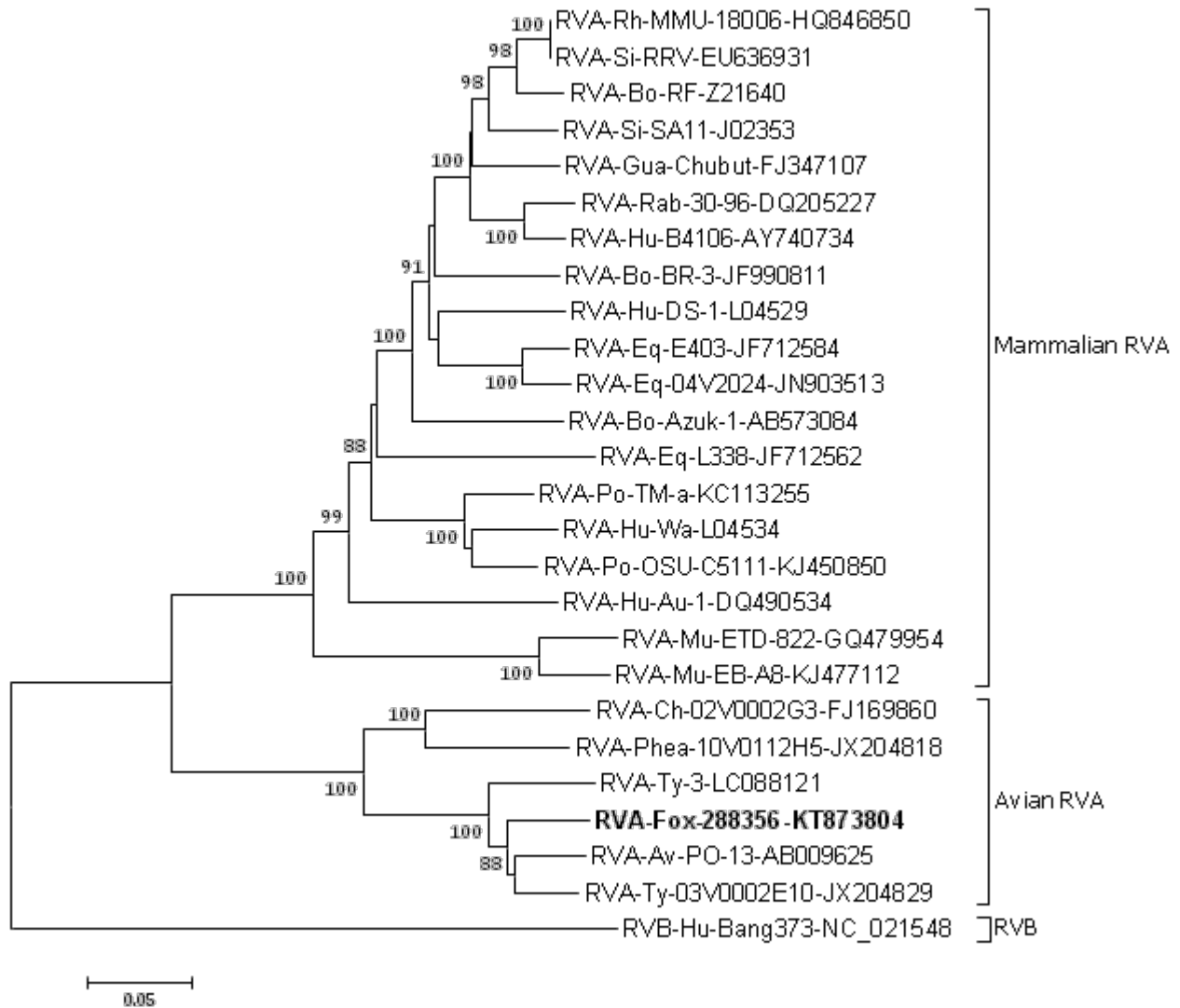
(F) VP7



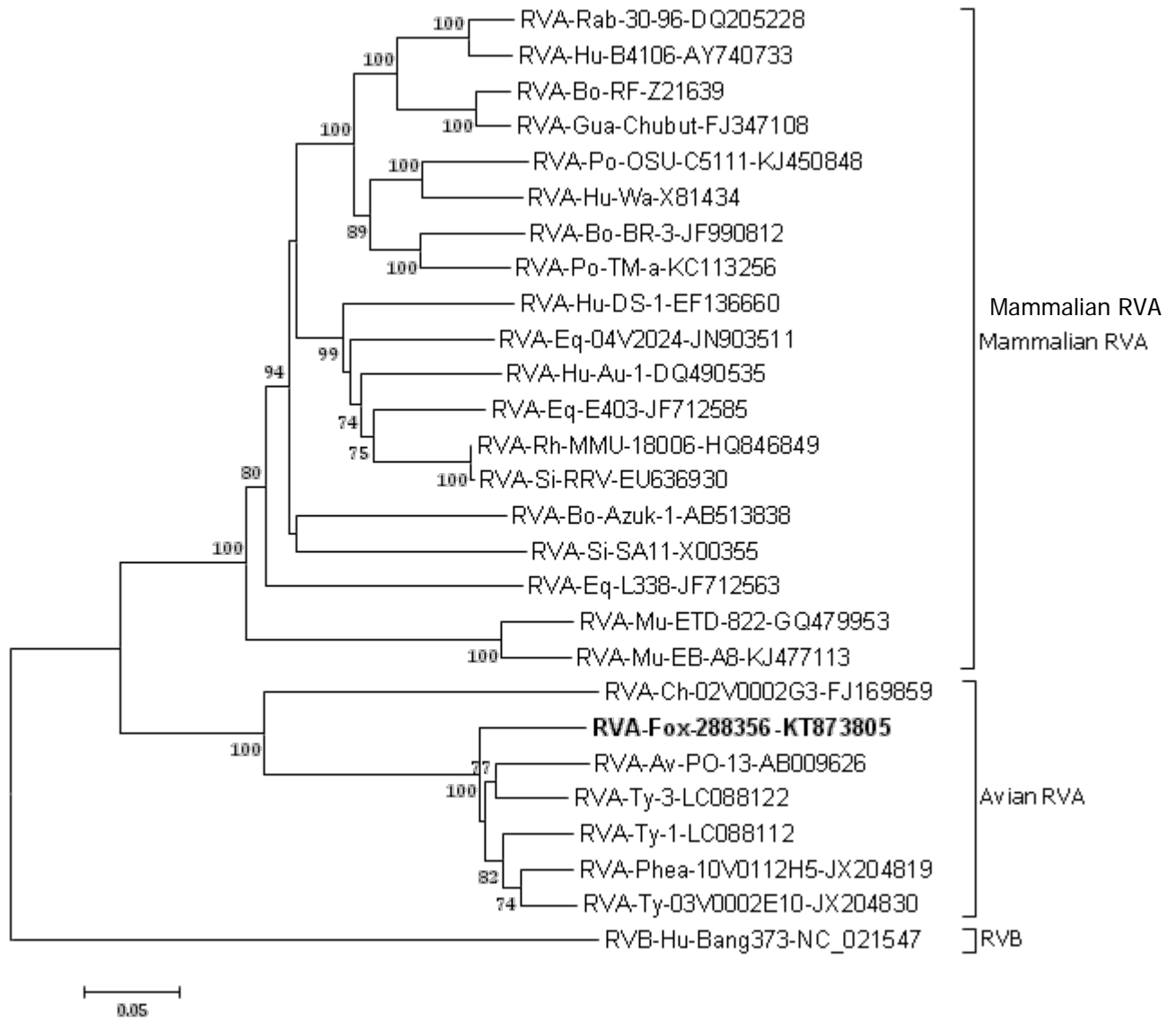
(G) NSP1



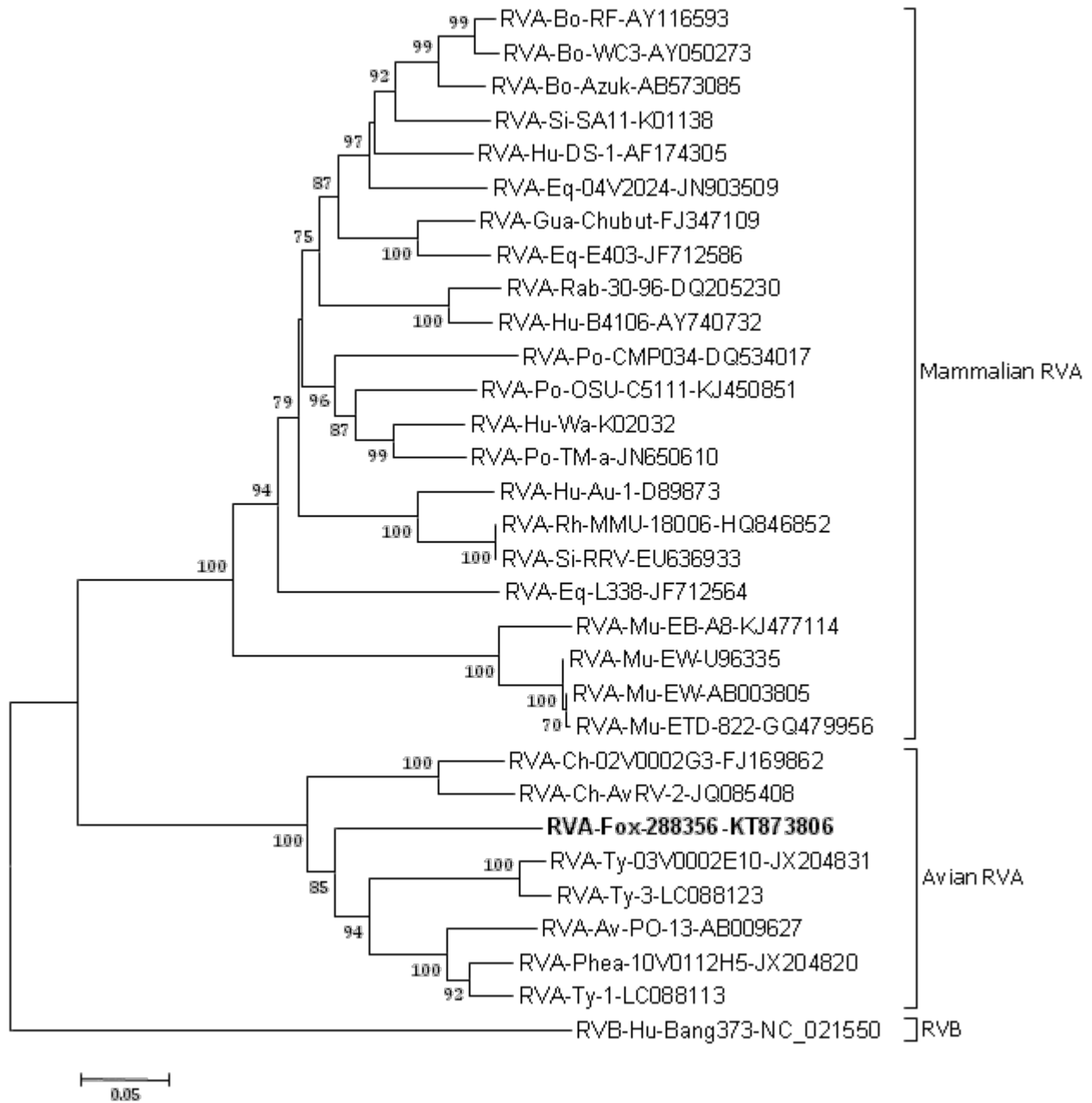
(H) NSP2



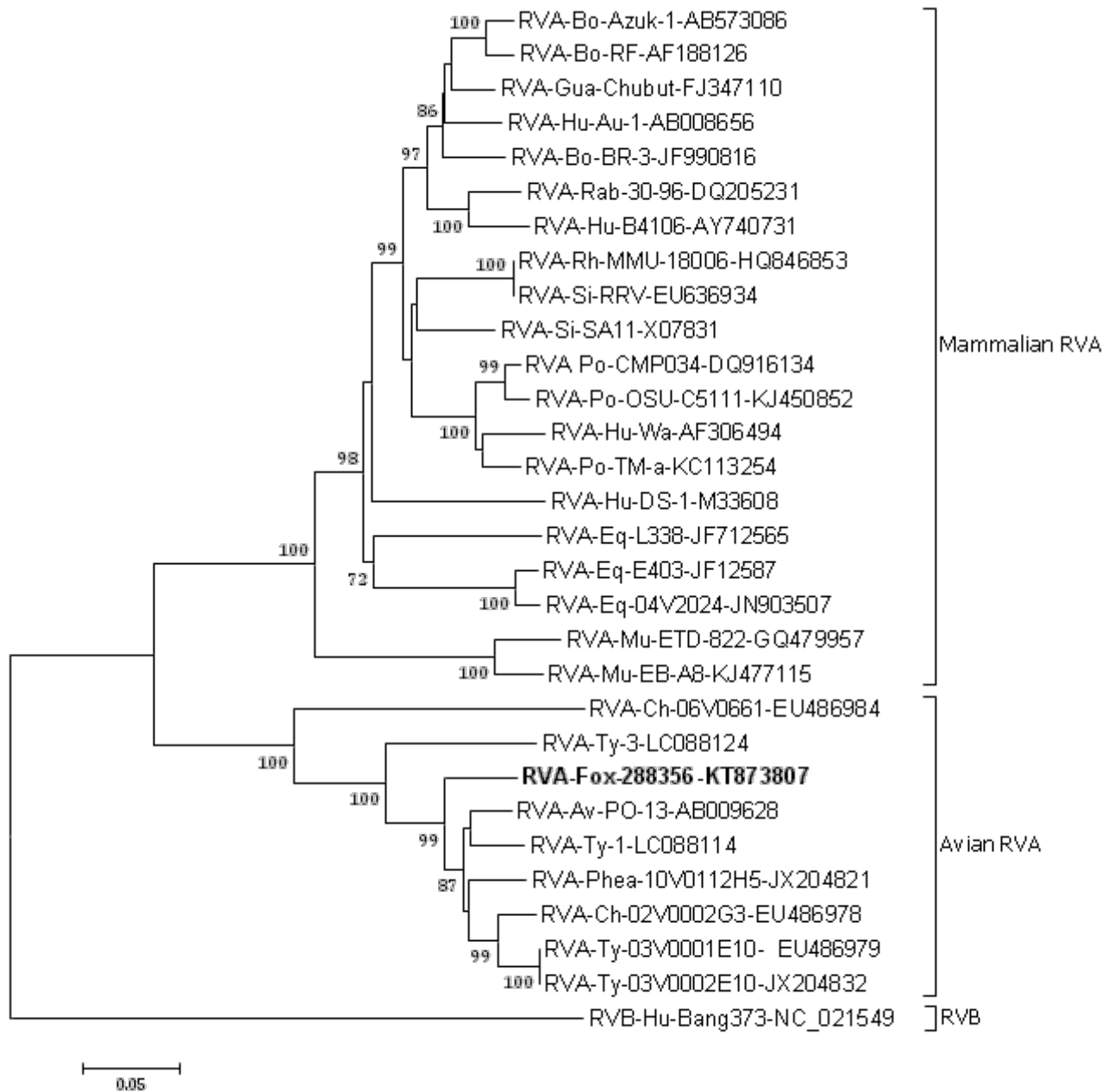
(I) NSP3



(J) NSP4



(K) NSP5



```

                10          20          30          40          50
VP7 288356    MYGTECTILL IEIIFYFFTA VVYDVIHKM ANSPTLCIIV LTIVFAASPK
VP7 PO-13     --S----- -A----- -A----- -IF--A- -AV---V---

                60          70          80          90          100
VP7 288356    CFAQNYGIDA PIIGSLDVTI PNKTNDQIGL VSSLCIYYPN EAETEINDTE
VP7 PO-13     -----NV --T-----AV ----D----- T----- -----N-
                                                    A

                110         120         130         140         150
VP7 288356    WKSTVAQLLL TKGWPTTSVY LNGYVDLQSF SNNPQLNCDY NIVLIKYNQN
VP7 PO-13     --D----- -----A----- -----V--D--

                160         170         180         190         200
VP7 288356    AGLDISELAE LLLYEWLCNE MDVRLYYYQQ TSEANKWIAM GRDCTIKVCP
VP7 PO-13     ----M----- -----N----- -A-----L-- -S-----
                                                    B

                210         220         230         240         250
VP7 288356    LNTQTLGIGC QTTNVATFEQ LTANEKLAII DVVDGVNHKI NYSVASCTIK
VP7 PO-13     ----- ---D----- ---T----- -----V --TI-T--L-
                                                    C

                260         270         280         290         300
VP7 288356    NCIRLNQREN VAIIQVGGPE IIDVSEDPMV VPKMIRATRI NWKKWWQVFY
VP7 PO-13     -----I-----

                310         320
VP7 288356    TVIDYINTII QAMSKRSRSL NASAYFLRV
VP7 PO-13     --V----- -T-T----I

```

Technical Appendix Figure 4. Alignment of the deduced amino acid sequence of VP7 from avian-like RV 288356 and avian rotavirus PO-13. Three potential N-linked glycosylation sites, labeled in red, are present in the Fox-288356 and PO-13 VP7 sequence. Only aa positions 72 and 321 were mapped to hydrophilic regions in Kyte and Doolittle hydrophathy plots. Antigenic regions A, B and C, involved in the determination of VP7 serotypes, are underscored. Within these three regions, Fox-288356 rotavirus differed from PO-13 in 7 aa. Identical residues are indicated by dashes.

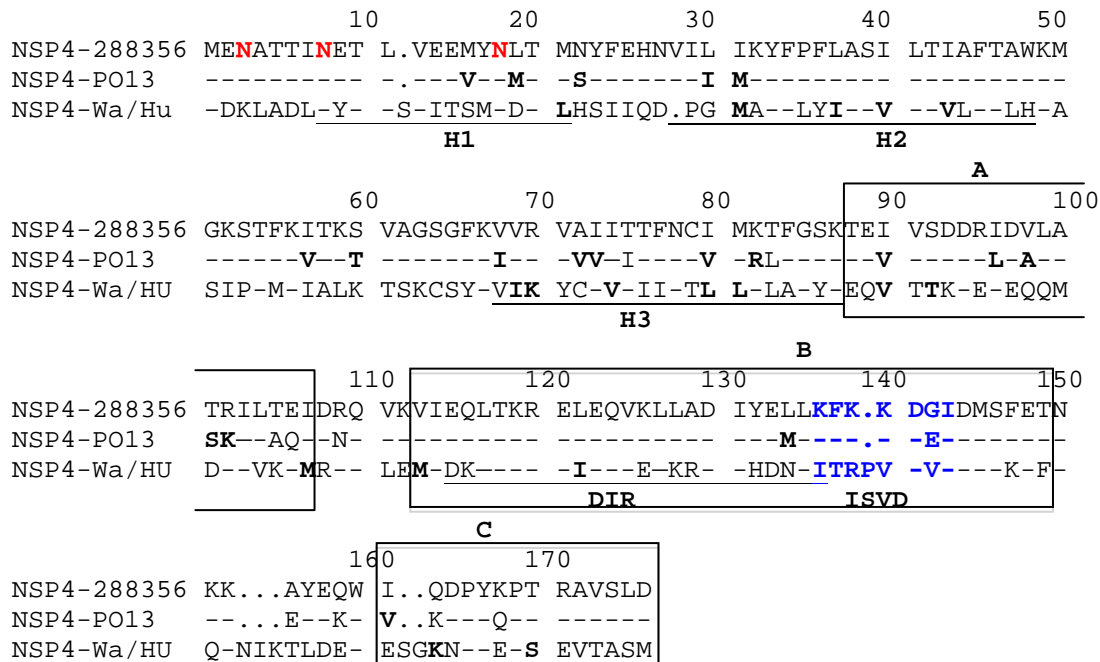
A

```
                210      220      230      240      250
VP4 288356  CNYIIIPKNQ TQQLEGFLKN GLPPIQESRY IMPVERLVQN IYQAKPNEDI
VP4 PO-13  -----V--S- ----D----- * -----S-- --R-----
                                     §      §
```

B

```
                310      320
VP4 288356  YERDGETVVA HTTCSVAGVN
VP4 PO-13  -----I-
```

Technical Appendix Figure 5. Alignment of VP4 amino acid sequences of functional regions from Fox-288356, avian PO-13 and Simian RRV rotavirus. (A) Two of the three arginine residues, important for the VP4 cleavage by trypsin in VP8 and VP5, are conserved in the PO-13 strain (amino acids 229 and 243 in PO-13 strain corresponding to 231 and 247 in RRV, respectively), and only one arginine is conserved in the amino acid sequence of Fox-288356 VP4 (amino acids in position 229), compared to mammalian rotaviruses. Identical residues are indicated by dashes. Arginine residues are indicated by asterisk in the trypsin cleavage regions and different residues are indicated by §. (B) The integrin ligand sequence motif (DGE) is conserved in avian rotavirus PO-13 and in Fox-288356 rotavirus as well as in most of the mammalian rotaviruses.



Technical Appendix Figure 6. Alignment of the NSP4 amino acid sequences encoded by Fox-288356, PO-13 and Human Wa strain rotaviruses. Two potential *N*-glycosylation sites are present at the same position as those of mammalian rotaviruses at position 8 and 17, and an additional third potential *N*-glycosylation site is present at amino acid position 3. Only two hydrophobic domains, corresponding to H2 (amino acids 27–47) and H3 (amino acids 67–85), out of the three present in mammalian rotaviruses, are present in Fox-288356 and PO13 strain. These two hydrophobic domains are not identical in Fox-288356 rotavirus compared to PO13 rotavirus: H2 shows two conservative aa exchanges at positions 29-30, H3 shows 5 conservative (position 67 -71 -72 -79 -81) and 2 non conservative (position 75 -82) aa exchanges. Among the five putative functional domains mapped on NSP4, the VP4-binding domain, in particular the diarrhea-inducing region (DIR), is conserved among Fox-288356, PO-13 and mammalian rotavirus; the InterSpecies Variable Domain (ISVD), between residues 131 and 140, exhibits a high degree of sequence variation and mutations, in particular at aa 131, 135 and 138, that are supposed to affect the virulence of the virus as well as the diarrhea-inducing and double-layered particle binding activities of the protein (9–11). Moreover, the ISVD of the Fox-288356 strain shows a non conservative substitution in aa 140 (140-Gly to Glu), compared to PO13 rotavirus. The oligomerization-associated domain (A), VP4-binding domain (B) and ss particle-binding domain are boxed. The hydrophobic domains are indicated as H1, H2 and H3. The potential *N*-glycosylation sites are in red. The Diarrhea-Inducing Region (DIR) is underlined. The InterSpecies-Variable Domain (ISVD) is in blue. Identical residues are indicated by dashes, conservative substitutions are indicated in bold and gaps are indicated by dots. When analyzing the inferred aa sequence in detail, the NSP4 of the fox isolate was six residues shorter than that of mammalian RVAs.